

AFM Operating-Drift Detection and Analyses based on Automated Sequential Image Processing

Zhikun Zhan^{1,3}, Yongliang Yang^{1,3}, Wen J. Li^{1,2,*}, Zaili Dong¹,

Yanli Qu¹, Yuechao Wang¹ and Lei Zhou¹

¹Robotics Laboratory, Shenyang Institute of Automation, Chinese Academy of Sciences, Shenyang, China

²Centre for Micro and Nano Systems, The Chinese University of Hong Kong, Hong Kong, China

³Graduate University of Chinese Academy of Sciences, Beijing, China

Abstract—Nanomanipulation and nanoimaging with Atomic Force Microscopes (AFM) is a popular technique for nanomanufacturing. However, under ambient conditions without stringent environment control, nanomanipulation tasks are difficult to complete because various system drift can cause uncertainties of the spatial relationship between the AFM probe tip and the nano-entities to be manipulated. Researchers have speculated that thermal drift is one of the major causes of errors for nanomanipulation using AFM systems, but to this date, quantitative analyses of AFM drift phenomenon are almost non-existent. This paper gives a detection and analyses method for AFM operating-drift based on automated sequential image processing, which provides a quantitative understanding of the AFM drift phenomenon. Essentially, the drift of an AFM system can be measured by a Phase-Correlation Method among consecutively scanned images. In order to eliminate the effects of z-direction drifts in x, y displacements, a gradient calculation method is introduced. The influence of a PZT actuator's thermal expansion on overall system drift is also analyzed. The results showed that although the length of the PZT actuator's expansion is the greatest among all the main system components, it may not be the main cause of the overall system drift.

Keywords—Atomic Force Microscopes (AFM); automatic nanomanipulation; automated sequential image processing; nanomanipulation drift

I. INTRODUCTION

Nanoscale imaging and manipulation are important technologies for fabricating novel nano-materials, discovering new physical phenomenon in the nano-world, and developing advanced nano-devices. However, there are still many challenges to be solved on nanoimaging and nanomanipulation. For example, when manipulating particles in nano-scale using an Atomic Force Microscopes (AFM), the spatial position of samples or the probe will drift during a manipulation process, if the AFM system is not in a stringently controlled environment. Therefore, extended human intervention is required to compensate for the spatial uncertainties associated with the AFM and its piezoelectric drive mechanism, such as hysteresis, creep, and thermal drift [1]. The latter is the major cause of spatial uncertainties in an AFM mechanical system due to thermal expansion and contraction [2]. The results of these components' expansion and contraction will cause the displacement of AFM probe or sample relative to their initially observed position even without any driving voltage applied to the piezoelectric drive mechanism. Such drift can seriously influence the perceived position of a nano-object during consecutively observed AFM scanned images. For example, Fig.1 (a) and (b) are the

scanned images of a nano-feature by an AFM at different time T1 and T2. Fig.1 (c) is an object image template which is cut out from (a) and can be matched in (b). By image processing, the object drifted from (2.87, 5.47) to (1.05, 6.29) in x, y directions of the sample frame (units in μm) during an interval of over five hours (the scanned area is $10 \times 10 \mu\text{m}$). Another example is the distortion phenomenon that occurs when a nano-object is scanned by an AFM in different ways. Fig.1 (d) and (e) show the same object in two consecutively scanned images but in different scanning directions. As shown, the modality of the object in the consecutive images is changed. Hence, factors that affect scanned image of a nano-object and the position of the nano-object should be quantitatively measured and compensated in order to enhance the reliability and repeatability nanoimaging and nanomanipulation tasks.

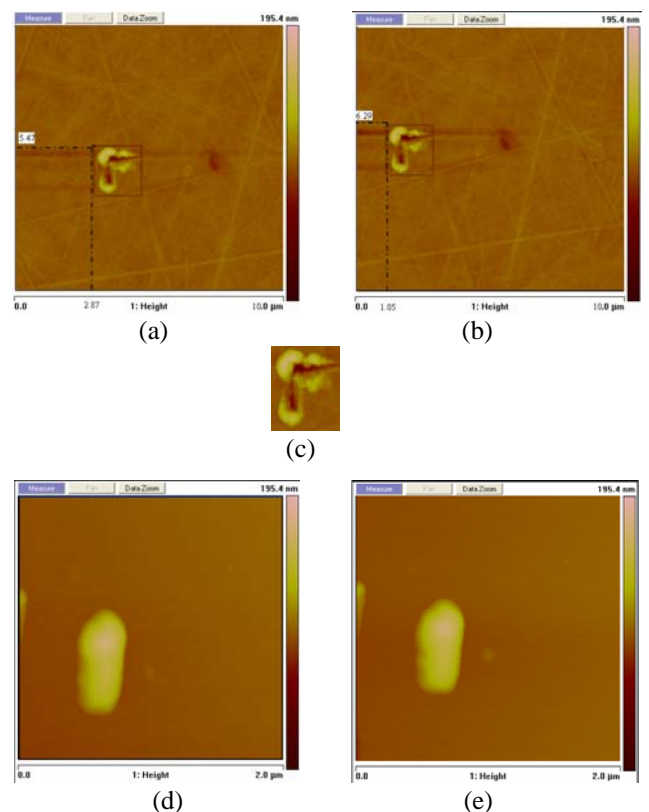


Fig. 1 An example of drift influences in nanomanipulation (a) and (b) are scanned image sequence of a scare on a CD disc; (d) and (e) are the scanned images of the same dot on a grating, but with different modality; (c) object template image.

*Contact author: wen@mae.cuhk.edu.hk; Wen J. Li is a professor at The Chinese University of Hong Kong and also an affiliated professor at The Shenyang Institute of Automation, CAS.

This project is funded by the Chinese National 863 Plan (Project code: 2006 AA04Z320) and the NSFC (Project code: 60635040 and 60675060).

Generally, these drifts and uncertainties are mainly caused by the nano-positioning actuators made of piezoelectric (PZT) materials. It is reported that a typical PZT thermal expansion coefficient is $1\sim 5 \times 10^{-5} / ^\circ\text{C}$. That means a one degree change of temperature will cause a 40~200 nm displacement in the length of the PZT actuator assuming its original length is 40mm.

Usually, the AFM vendor can offer some methods to improve the PZT nonlinearities such as hysteresis and creep. The former can be reduced by keeping scanning in the same direction, while the latter can be eliminated by waiting a few minutes after each large scanning motion [2].

Many researchers have explored methods for drift compensation. Several authors have developed simple approaches [3][4][5], in which the drift velocity was assumed to remain constant. However, such assumption has a large drawback since the drift is generally not linear. Mokaberi et al., had estimated drift by Kalman filtering techniques, and developed a compensator [2] [6]. But it is difficult for a user to select a tracking window and appropriate model parameters to adapt the change of operating environmental conditions [1]. Yang et al., proposed a compensation scheme based on block phase correlation, and they estimated the drift at the next sampling interval using Neural Network and designed a real-time controller for nanomanipulation as if drift does not exist [1] [7].

Our group is working on using image processing and analyses as tools to measure and analyze AFM system drift during nanomanipulation and nanoimaging procedures. Image registration technique has already been proven as an important technology for recognizing and tracking objects in macro and micro scale objects. For example, *correlation method* is one means of image registration that calculates correlation value among the images directly in spatial domain. Other available methods can also be used to calculate correlation value in frequency domain, e.g., fast Fourier transform-based (FFT based) Phase-Correlation Method (PCM) [8]. PCM is a common method used to match image translation, rotation, and scale with respect to one another. PCM is also effective when two images have differences due to noise and asymmetric illumination.

In this paper, the Phase-Correlation method used to measure the drifts of sample is discussed, and some analyses of the drift characteristics during the operations of an AFM are presented. In addition, the approach to eliminate z-drift influence and distortion of the scanned object image are introduced.

II. DRIFT DETECTION

A. AFM imaging transformation

AFM scanned images are reconstructed from topographic data which represent the height information of discrete points on sample surface, i.e., the different colors in scanning images show different height of the sample topography. As the image color changes, the drift of z direction can be inferred during AFM operation. Fortunately, the drift in z direction can be considered as having little correlation to x-y plane. Hence, the

z-drift influence can be eliminated by transforming the original scanned images to gradient ones [5].

To eliminate the z-drift influence, we use the method as follows. First, the two scanned height data of AFM at time k and $k+1$ can be written as

$$h_{k+1}(x, y) = h_k(x + \Delta x_k, y + \Delta y_k) + \Delta z_k \quad (1)$$

Here, $\Delta x_k, \Delta y_k, \Delta z_k$ denote drift in the x, y and z directions respectively, between the two time k and $k+1$.

The x-direction gradient can be computed as

$$g_{kx}(x, y) = h_k(x, y) - h_k(x-1, y) \quad (2)$$

Similarly, the y-direction gradient can be computed as

$$g_{ky}(x, y) = h_k(x, y) - h_k(x, y-1) \quad (3)$$

Substituting (1) into (2) and (3), we can get

$$g_{kx+1}(x, y) = h_{k+1}(x, y) - h_{k+1}(x-1, y) \\ = h_k(x + \Delta x_k, y + \Delta y_k) + \Delta z_k - (h_k(x + \Delta x_k - 1, y + \Delta y_k) + \Delta z_k) \quad (4)$$

$$= g_{kx}(x + \Delta x_k, y + \Delta y_k)$$

$$g_{ky+1}(x, y) = h_{k+1}(x, y) - h_{k+1}(x, y-1)$$

$$= h_k(x + \Delta x_k, y + \Delta y_k) + \Delta z_k - (h_k(x + \Delta x_k, y + \Delta y_k - 1) + \Delta z_k) \quad (5)$$

$$= g_{ky}(x + \Delta x_k, y + \Delta y_k)$$

Then, the drift in z-direction is eliminated.

Our experiments showed that using Phase-Correlation Method to measure the displacement of two gradient images is more effective than using the original images. Furthermore, in two consecutive gradient images, there are no topography changes. Fig. 2 shows the original scanned images and gradient (x-direction) images of a standard reference grating with a scan size of 10×10 microns. The right image of Fig. 2 (a) was scanned over several hours later comparing with the left one (original image).

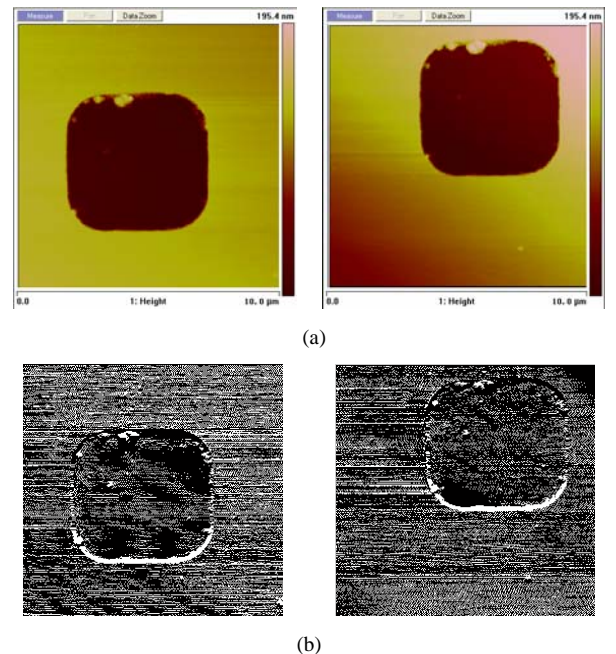


Fig. 2 (a) AFM Scanned images of a standard reference grating. (b) gradient images of (a).

B. Phase-Correlation Method based on gradient

Here, the Phase-Correlation Method used to measure the displacement between images is given. Using the shift property of Fourier Transform, phase correlation method can transform a shift in spatial domain to a phase difference in the frequency domain.

We can describe a pair of consecutive images as $h_k(x, y)$ and $h_{k+1}(x, y)$, and their gradients are $g_k(x, y)$ and $g_{k+1}(x, y)$ respectively, as mentioned above in equation (1)-(5).

The Fourier transformation of $h_k(x, y)$ and $h_{k+1}(x, y)$ are $H_k(f_x, f_y)$ and $H_{k+1}(f_x, f_y)$. Assuming that there is a displacement $(\Delta x, \Delta y)$ between the two consecutive images, using the shift property of Fourier Transform, the relationship between the two Fourier transformations of images is written as

$$H_{k+1}(f_x, f_y) = H_k(f_x, f_y) \exp[-j2\pi(\Delta x f_x + \Delta y f_y)] \quad (6)$$

The cross correlation function of the two frames is

$$c_{k,k+1}(x, y) = \xi^{-1}(H_k^*(f_x, f_y) H_{k+1}(f_x, f_y)) = \delta(x - \Delta x, y - \Delta y) \quad (7)$$

In order to eliminate the z-direction drift, gradient images are used here. Then (7) can be rewritten as

$$c_{k,k+1}(x, y) = \xi^{-1}(G_k^*(f_x, f_y) G_{k+1}(f_x, f_y)) = \delta(x - \Delta x, y - \Delta y) \quad (8)$$

In (8) above, $G_k(f_x, f_y)$ and $G_{k+1}(f_x, f_y)$ are the two-dimensional discrete Fourier transform of $g_k(x, y)$ and $g_{k+1}(x, y)$ respectively. ξ^{-1} denotes inverse Fourier transform and $*$ denotes complex conjugate. Equation (7) is also an impulse function in the x-y plane, and the position is an estimate of the drift between the two consecutive frames.

III. Drift Characteristics Analyses

A. Spatial Analyses

Here we assume that the AFM drift can be described as the displacement between the probe frame and the sample frame. Three coordinate frames can be defined in a typical AFM system as shown in Fig. 3. They are the base frame $O_B(x_B, y_B, z_B)$, the sample frame $O_S(x_S, y_S, z_S)$ and the tip frame $O_T(x_T, y_T, z_T)$.

During an AFM scanning process, the tip is driven by a PZT actuator. Once a voltage is applied to the actuator, the PZT actuator will move in the corresponding direction. As discussed in Section I, even without changing the applied voltage to drive the PZT, the tip may drift with respect to the base frame. So, we can describe the relationship between the tip frame and the base frame as follows:

$$O_T = O_B + T_{TB} \quad (9)$$

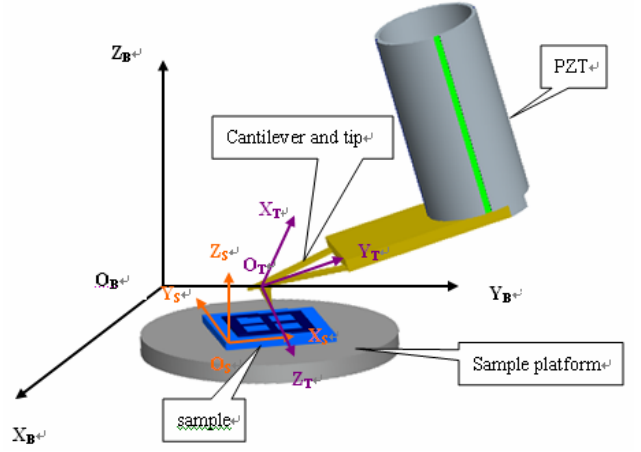


Fig. 3 An illustration of a typical AFM scanning system with 3 defined coordinate frames.

Here,

$$T_{TB} = (t_{BX} \quad t_{BY} \quad t_{BZ})^T$$

is the translation vector. If we ignore (or compensate for) the hysteresis, creep, and non-linearity of the displacement-voltage curve, the translation will be composed of two parts: one is the piezo extension E_p ; the other is drift D_{TB} of the tip relative to the base frame, that is

$$T_{TB} = E_p + D_{TB} \quad (10)$$

The transformation relationship of the sample frame and the base frame can be written as

$$O_S = O_B + T_{SB} \quad (11)$$

And,

$$T_{SB} = (t_{SX} \quad t_{SY} \quad t_{SZ})^T$$

is the translation vector which contains only drift D_{SB} between the sample and the base frames. By vector computation, the relationship of frame O_S and frame O_T can be derived as:

$$O_S = O_T + T_{SB} - T_{TB} \quad (12)$$

The transformation describes the respective position change of samples and the tip, which can effects the topography map during the scan-imaging by AFM.

B. Statistical properties analyses

The drift during AFM scanning is the result of several factors such as temperature, humidity, working characteristics of PZT as well as other unknown causes. As operation time passes, the displacement caused by system drift will increase significantly. The desired nano-object of interest will possibly move out of the scanning area when the drift exceeds the scanning range. This phenomenon can seriously influence nanoimaging and nanomanipulation tasks. Hence, drift measurement and compensation are important to keep AFM operations stable and reliable. We have measured the average drift velocities of a sample placed in our SPM system (Veeco Dimension 3100). The drift velocity tends to vary from 1.5 ~

5.4nm/min in x-direction on tapping mode scanning. For example, a sample region that will be out of the $1 \times 1 \mu\text{m}$ scanning area needs to take 185~667 minutes in room temperature ($20 \pm 2^\circ\text{C}$).

The behaviors of AFM drift are usually random as operation time passes, which is partly due to the environmental condition changes such as temperature, humidity, vibration. Fig. 4 shows measurement of drift in x and y directions of our AFM over 3 hours. Fig. 5 shows the corresponding drift velocity curve, from which we can find that drift velocities are not linear.

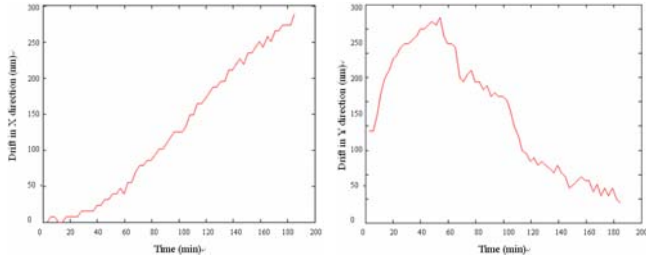


Fig. 4 Measurement of drift in x and y directions over 180 minutes.

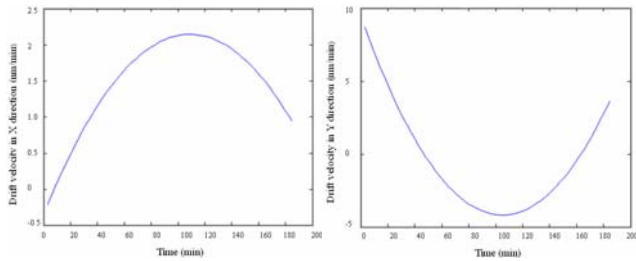


Fig. 5 Drift velocity curve in x and y directions.

Thermal drift is the greatest uncertainty factor. Generally, the heat to cause the temperature change of the scanner mainly comes from the components contained in an AFM system when environmental temperature is controlled strictly. Since the mechanical swing and vibration of PZT actuator are typically in a high frequency (over a few decades of Hz in x, y directions and at least several kHz in z direction), hence it is entirely possible that heat is constantly being released in the scanning area of an AFM. Fig. 6 gives the temperature variation curve of a PZT actuator during 3 hours of operation, i.e., with an applied AC voltage of 78~118 ppV, 71Hz in x-direction. (Note that this experiment was performed on a typical PZT nano-actuation tube, and not directly on the Veeco's PZT actuator as it is enclosed in a protective shell within the AFM system.) As shown, the temperature increased 1.6°C over 3 hours.

As mentioned earlier, AFM drifts are the integration results of several factors, but thermal changes is a main one. As shown in Fig. 3, there are several key components within the AFM enclosure during an operational procedure, i.e., PZT actuator, cantilever-tip (silicon nitride), grating sample (silicon) and sample platform (steel), which can influence the relative position between the tip and samples. Table 1 shows the mechanical length variations due to thermal expansion by 1.0°C change in temperature (assuming that the original areas of sample platform and grating are the scanning region). The data of Table 1 indicates that with 1.0°C change in temperature, the

total length extension of the PZT actuator is the greatest compared to other components, and therefore could be the most dominating factor in the overall system drift. However, by comparing the data of Fig. 4 and Fig. 6, it is obvious that although the thermal drift is one important factor for AFM systems drift, but is not the only factor, as the curve trends in Fig. 4 do not follow the curve trend in Fig. 6.

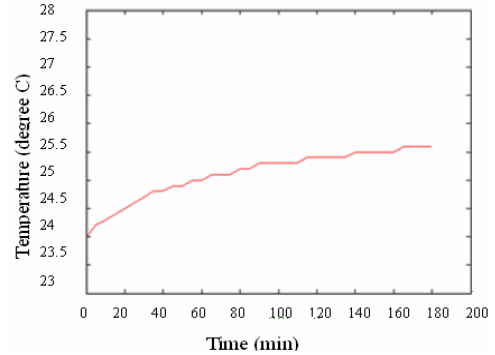


Fig. 6 Temperature curve of a typical PZT actuated over 3 hours.

IV. PCM ANALYSES ON VEECO SPM SYSTEM

We have conducted several drift analyses experiments on a Veeco AFM/SPM system (Veeco Dimension 3100). The scanning sample is a standard grating, and the referent target object is a $\sim 300 \times 300\text{nm}$ feature on the grating. Fig. 7 shows four representative images extracted from a scanning sequence of images during a 3 hour operational time. The scan rate used was 1.5Hz which corresponds to an imaging frequency of 0.006 Hz . Each scanned image is 256×256 pixels and represents a $2 \times 2 \mu\text{m}$ area of the sample surface. By using the Phase-Correlation Method and gradient calculation method on the sequence of images, the displacement of the referent target were calculated in x, y directions of the operation frame. The displacement of the target implies the drifts of the AFM system during its operation period. The temperature of the ambient temperature was recorded as well during the experiments.

Fig. 8 shows the results from 2 different scanning experiments, with drift results in x and y directions for each experiment. The temperature variations during these scanning experiments are also included in the figure for comparison. The experiments were conducted with the same settings of scan rate, scan size, scan angle and so on. We have actually conducted many experiments and these 2 experimental results represent the general scanning drift characteristics of our AFM system.

All experiments showed that there is little correlation between the drifts in x and y directions and that the drift in x-y plane can be considered as a translation movement, i.e., no rotational coupling. The displacement among the target scanning image sequence were calculated by Phase-Correlation Method and the measurement resolution of the displacement is about 8-10nm when the scanning size is $2 \times 2 \mu\text{m}$. The environmental temperature is in the rage of $20 \sim 22^\circ\text{C}$.

Table 1. Comparison of length expansion due to increase of 1°C of temperature.

AFM components and material	Piezoactuator (PZT)	Cantilever-tip (silicon nitride)	Grid (silicon)	Sample Platform (steel)
Linear thermal expansion coefficient (/K)	$1\sim 5\times 10^{-6}$	3×10^{-6}	2.6×10^{-6}	1.2×10^{-5}
Original length (μm)	40,000	134	10	10
Change in length (nm/K)	40~200	8.4×10^{-2}	1.82×10^{-2}	28.2×10^{-2}

From the figure, we again conclude that the drift of the AFM system does not totally depend on the temperature change of the system during its operation, i.e., the thermal expansion of the PZT actuator is not the only dominating factor causing the overall system drift. Further investigation should be carry out to understand other factors that affect the AFM drift phenomenon.

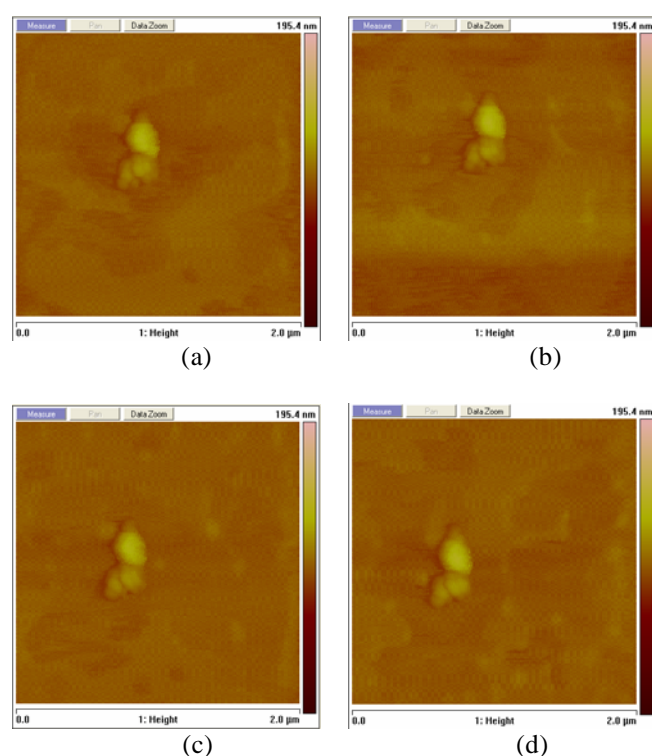


Fig. 7 scanned image of the target nano-object ($\sim 300\text{nm}\times 300\text{nm}$) on a standard grating in our Veeco AFM/SPM system experiments.

V. CONCLUSIONS

This paper provides a quantitative discussion of the AFM system drift phenomena during its operations. The measurement approach based on *phase-correlation* and *gradient calculation* methods are described. The processing and analyses of the experimental data are presented.

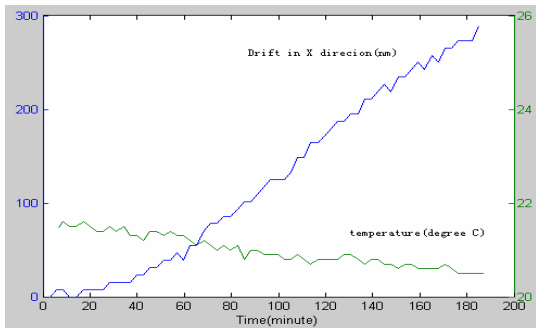
By using the shift property of Fourier Transform, the Phase-Correlation Method can be used to obtain the displacement of the referent target given a sequence of

images. Using this method, accurate measurement of the drift displacement can be obtained efficiently. In order to eliminate the z-drift influence to the x-y plane in topographic images, the gradient modes of original images were used. We note here that the experiments were conducted on a Veeco AFM/SPM system, so the results presented in this paper may not be the same for other AFM/SPM systems.

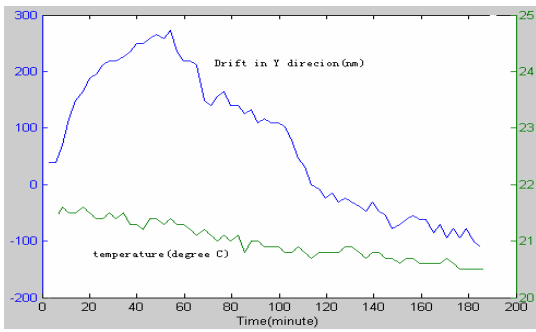
The *drift* of an AFM system is a quite complex phenomenon during nanoimaging and nano-manipulation procedures. Much more research should be performed to further understand and compensate it in the future.

REFERENCE

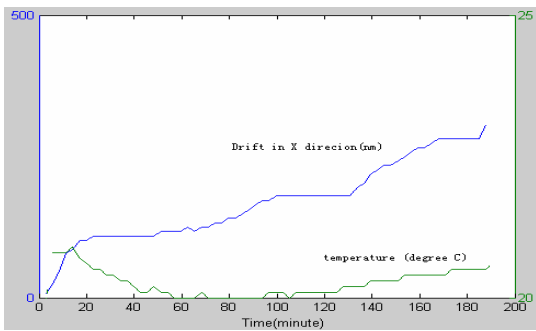
- [1] Q. Yang, S. Jagannathan and E. W. Bohannon, "Block phase correlation-based automatic drift compensation for atomic force microscopes", IEEE Int. Conf. on Nanotechnology, Nagoya, Japan, July 2005.
- [2] B. Mokaberi and A. A. G. Requicha, "Towards automatic nanomanipulation drift compensation in scanning probe microscopes", IEEE Int. Conf. on Robotics and Automation, New Orleans, LA, April 25-30, 2004.
- [3] K. J. Ito, Y. Uehara, S. Ushioda and K. Ito, "Servomechanism for locking scanning tunneling microscope tip over surface nanostructures", Rev. of Sci. Inst., Vol. 71, No. 2, pp. 420-423, February 2000.
- [4] R. Staub, D. Alliaia and C. Nicolini, "Drift elimination in the calibration of scanning probe microscopes", Rev. Sci. Inst. Vol. 66, No. 3, pp. 2513-2516, March 1995.
- [5] V. Y. Yurov and A. N. Klimov, "Scanning tunneling microscope calibration and reconstruction of real image: Drift and slope elimination", Rev. Sci. Inst., Vol. 65, No. 5, pp. 1551-1557, May 1994.
- [6] B. Mokaberi and A. A. G. Requicha, "Drift compensation for automatic nanomanipulation with scanning probe microscopes", IEEE Trans. on Automation Science and Engineering, Vol.3, NO.3, July 2006.
- [7] Q. Yang and S. Jagannathan, " Nanomanipulation using atomic force microscope with drift compensation", Proceedings of the 2006 American Control Conference, Minneapolis, Minnesota, USA, June 14-15, 2006.
- [8] B. Strinivasa Reddy and B. N. Chatterji, " An FFT-Based Technique for Translation, Rotation, and Scale-Invariant Image Registration," IEEE Transactions on Image Processing, Vol.5, NO.8, August 1996.



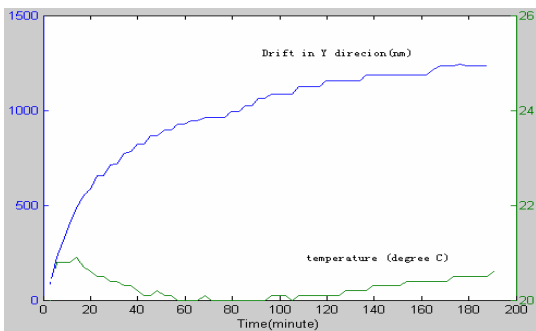
(a)



(b)



(c)



(d)

Fig. 8 Curves of the target drift measurement and the environmental temperature. (a) and (b) are from the first set experiment (same set as data as shown in Fig. 5). (c) and (d) are from a different set of experiment.